Energy and AI 13 (2023) 100270

Contents lists available at ScienceDirect

Energy and AI

journal homepage: www.elsevier.com/locate/egyai

Applying machine learning techniques to predict laminar burning velocity for ammonia/hydrogen/air mixtures

Cihat Emre Üstün [a,*], Mohammad Reza Herfatmanesh [a], Agustin Valera-Medina [b], Amin Paykani [a]

[a] School of Physics, Engineering and Computer Science, University of Hertfordshire, Hatfield, AL10 9AB, United Kingdom
[b] College of Physical Sciences and Engineering, Cardiff University, Cardiff, CF24 3AA, United Kingdom

GRAPHICAL ABSTRACT

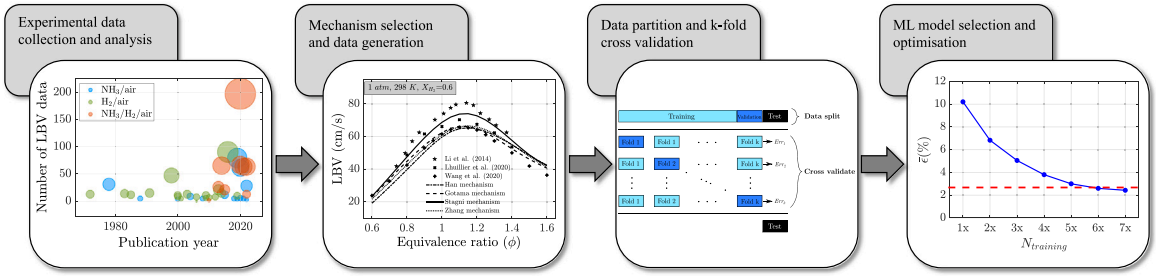

HIGHLIGHTS

- ML-based prediction of LBV for ammonia/hydrogen/air mixtures is presented.
- Comparative performance analysis of 24 ML algorithms is studied.
- GPR achieves the highest accuracy for LBV velocity prediction.
- ML model can predict LBV up to 27000 times faster compared to 1D simulations.

ARTICLE INFO

Keywords:
Machine learning
Ammonia
Hydrogen
Laminar burning velocity
Combustion

ABSTRACT

Ammonia utilisation in internal combustion engines has attracted wide interest due to the current trend toward decarbonisation, as ammonia is a zero-carbon fuel with different combustion properties to hydrocarbons. The laminar burning velocity (LBV) is a fundamental property of fuels with a significant effect on the combustion processes and accurate calculations and measurements of the LBV over a wide range of fuel blends, pressures and flow conditions is a time-consuming, complicated procedure. The main goal of the current study is to predict the LBV of NH_3/H_2/air mixtures using a hybrid machine learning (ML) approach based on a training dataset consisting of both the experimental LBV values and additional data obtained from numerical simulations with a detailed kinetic model. Initial ML model training data is collected from existing experimental LBV in the literature for NH_3/H_2/air mixtures. Then, synthetic data is generated using one-dimensional (1D) simulations to reduce data inhomogeneity and increase accuracy of the ML model. In total, 24 different ML algorithms are tested to find the best model both for the experimental and the hybrid dataset. The results suggest that both Gaussian Process Regression (GPR) and Neural Networks (NNs) can be utilised to predict LBV of NH_3/H_2/air mixtures with reasonable accuracy. The hybrid ML model achieved a coefficient of determination of $R^2 = 0.998$. Finally, hybrid ML model hyperparameters are optimised to achieve a coefficient

* Corresponding author.
E-mail address: c.e.ustun@herts.ac.uk (C.E. Üstün).

https://doi.org/10.1016/j.egyai.2023.100270
Received 16 March 2023; Received in revised form 3 May 2023; Accepted 6 May 2023
Available online 10 May 2023

of determination of R^2 = 0.999. It was also found that ML can speed up LBV computation from 9500 to 27000 times compared to 1D simulations with a reduced mechanism.

1. Introduction

Future propulsion and power generation technologies should use non-carbon energy sources combined with advanced high-efficiency energy conversion devices to meet net-zero carbon emissions targets. Carbon-free ammonia (NH_3) is among the most promising hydrogen carriers, thanks to its developed production and distribution infrastructure [1]. As a fuel, NH_3 has poor combustion properties such as low burning velocity, narrow flammability limit, high NOx emission, and a high auto-ignition temperature that can be improved by the addition of hydrogen (H_2), which can be obtained energy-efficiently by partially cracking ammonia into H_2 and N_2 prior to the combustion process [2]. The NH_3/H_2 blend will have a higher flame speed with significantly improved flame stability. It has been shown that very lean ammonia-hydrogen-air mixtures have the strong potential of fuelling of future internal combustion (IC) engines and gas turbines [3].

One of the most fundamental and significant combustion properties of a fuel is its laminar burning velocity (LBV), which is directly influenced by its diffusivity, exothermicity, and reactivity. It gives an indication of a fuel's overall reactivity, aids in calculating heat release rates, and validates detailed and reduced combustion reaction mechanisms. LBV is used in the description of the turbulent flame structure and speed, flame front instabilities, flame extinction via heat loss and stretch, and flame stabilisation [4]. Most importantly, computational fluid dynamics (CFD) for combustion simulations requires quick and precise prediction of LBVs under various combustion conditions. There are two main ways to obtain LBV: experiments and one-dimensional (1D) modelling. Experimental LBV measurements are often carried out using constant pressure and volume combustion chambers (CPCC, CVCC) with spherical flame (SF) method, particle tracking velocimetry (PTV), cylindrical bombs (CB), burner method (BM) with conical flames (CF) and heat flux burners (HFB), the details of these methods are discussed in detail in [4]. Another way to obtain LBV is to use 1D simulations with codes such as Cantera [5], Chemkin [6] and Opensmoke++ [7]. Chemical kinetic mechanisms are employed to compute LBV using 1D simulations. The accuracy of these simulations depends on the chemical kinetic mechanism size, stiffness and numerical setup. Additionally, these mechanisms are usually validated only for a narrow range of operating conditions and specific fuel mixtures. On the other hand, LBV can also be obtained by using developed empirical correlations that are usually based on the power-law. These correlations are usually developed using regression analyses on available experimental data. For NH_3/H_2/air mixtures, there are only two correlations available in the literature [8,9]. Goldmann et al. [8] developed LBV correlations using Mathieu and Petersen mechanism [10], for NH_3/H_2/air mixtures covering 0–100 vol% NH_3, 0–60 vol% H_2, $0.5 < \phi < 1.7$, 300 K < T < 1000 K and 1 bar < p < 250 bar. This correlation was then optimised and validated for fuel H_2 fractions less than 50% [11]. Later, Pessina et al. [9] developed correlations for NH_3/H_2/air mixtures only for full-load spark-ignition (SI) engine conditions, thus it is valid only in the range of p = 40–130 bar, T = 720–1208 K, and ϕ = 0.4–1.5. Developed correlation relies solely on chemical kinetics simulation data that was obtained using Stagni mechanism. which was chosen after a comparative mechanism selection study with Shrestha [12], Gotama [13], and Otomo [14] mechanisms. Developed correlation resulted in an average error of 2.5% and a maximum error of 16%.

The current advancements in machine learning (ML) along with increasing data volume, advances in computational resources, and data storage technologies for large datasets present new prospects for data analysis in combustion applications [15–18]. Recently, supervised ML algorithms attracted interest as another way to predict LBV of various fuels. Currently, there are only a limited number of studies on the application of ML for the prediction of LBV of fuels. In one of the first attempts, Mehra et al. [19] carried out experimental LBV measurements of CO and H_2 enriched natural gas (HyCONG) under normal temperature and pressure (NTP) conditions and developed an ANN model based on obtained LBV data. The developed model exclusively relied on one small experimental data source which increased the uncertainty of the model predictions. Furthermore, the model could only be applied to mixtures under NTP conditions. Later, Malik et al. [20] used deep neural networks (DNN) to predict LBV of H_2/air and C_3H_8/air mixtures for the first time. The dataset was randomly sampled from available experimental data to have sufficient training data. Even though the model performed well for a wide range of temperature and equivalence ratio conditions, the model was only validated for near atmospheric pressure conditions. Ambritus et al. [21] used DNN to estimate LBV of H_2/air mixtures. The study used both experimental and interpolation-based synthetic data to train the model. The results were compared with Malet correlation [22] for validation. It was reported that the non-homogeneity of the experimental dataset caused lower prediction accuracy and requires further experimental measurements. In another study, vom Lehn et al. [23] studied the use of artificial neural networks (ANN) for the prediction of LBV of various molecular combinations of a wide range of pure hydrocarbon and oxygenated hydrocarbon fuels. The dataset consisted of experimental LBV data of 124 fuel compounds and additional data generated by 1D numerical simulations using a detailed chemical kinetic mechanism, with a total number of 3444 data points. The study concluded that ML can be used for fuel design with reasonable prediction accuracy. The accuracy of ANN was confirmed by Eckart et al. [24] in their study, in which different ML models were compared for the LBV prediction of H_2/CH_4/air. It was concluded that the performance of the ANN model was found to be comparable to that of the GRI 3.0 mechanism. However, the ANN model was a little less accurate but much less computationally costly. Depending on the choice of input parameters and data structure, other ML models can outperform ANN. Wan et al. [25] developed a data-driven ML model based on available experimental data for HC and oxygenated fuels. In total, 5 descriptors calculated from semi-empirical quantum chemistry methods (Pearson correlation matrix) were used as model inputs. In total, 16 models were evaluated based on errors (R^2, MAE, RMSE, MSE). It was found that GPR algorithm with squared exponential kernel was the best-performing model. However, the study lacks validation of high-pressure and high-temperature conditions. Varghese and Kumar [26] developed an empirical model (power-law correlation) to predict LBV of syngas–air mixtures. The power-law correlation model was based on a multiple linear regression and model parameters (temperature and pressure components) were trained using ML. The model used data from experimental data as well as 1D glass-box model computations. It was reported that the predictions using the developed empirical model had an error margin of less than 10%. Recently, Shahpouri et al. [27] studied the ML-based laminar flame speed prediction of low-carbon fuels such as NH_3, H_2, CH_3OH and their combinations. The study uses 1D simulations to generate a large LBV database and then train the models using ANN and SVM algorithms. It is claimed that the models have a prediction capability for engine-relevant conditions, however, the validity of the predictions is rather unknown since no experimental measurements are able to verify this claim currently.

Existing literature often does not thoroughly discuss ML algorithm selection and optimisation, and the effect of training dataset size on accuracy. Furthermore, only a fraction of the studies focuses on zero-carbon fuels such as NH_3 and H_2 that are promising to replace HC fuels. The novelty of the current study lies in the use of ML algorithms for predicting the LBV of NH_3/air, H_2/air and NH_3/H_2/air mixtures based on

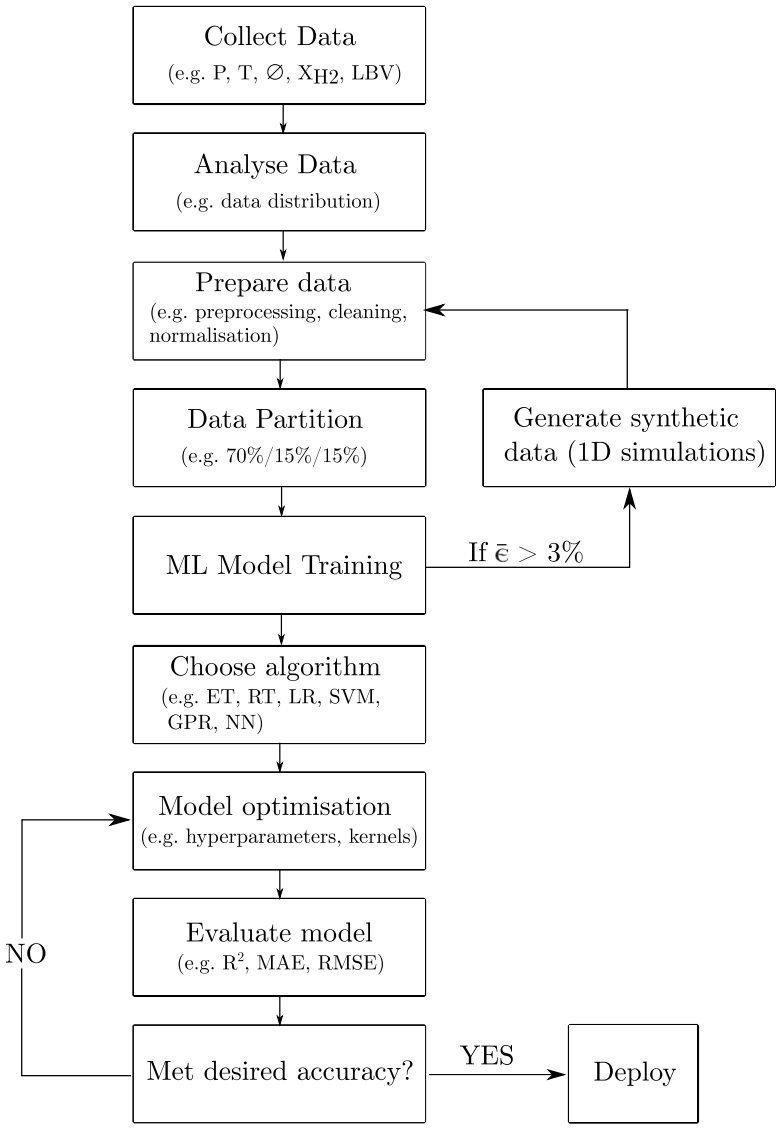

Fig. 1. Flowchart of the hybrid ML model development methodology.

a relatively small experimental dataset, as well as in finding the optimal dataset size and ML algorithm. The ML model is then improved via a hybrid approach that utilises additional LBV data from 1D simulations, resulting in increased accuracy. The remainder of this paper is divided into three sections. Section 2 defines the methodology, including the data collection and generation for training, model training approach and model validation. Section 3 evaluates the validity of the results, input feature dependencies, and comparisons with experimental data. Finally, Section 4 provides final remarks on the findings and future directions of research.

2. Methodology

In the present work, different ML algorithms are trained to predict LBV of NH_3/H_2/air mixtures which take on the initial temperature, initial pressure, equivalence ratio, and hydrogen content as input parameters. In this section, the experimental training dataset is introduced first, followed by a discussion on the availability of sufficient experimental measurements. Then, synthetic data generation, ML model training methodology, model evaluation metrics, and model optimisation are discussed. An overview of the methodology used in the development of the final ML model is given as a flowchart in Fig. 1. First, LBV data collected from the literature is analysed. Then the initial ML model is trained based on the experimental dataset. Synthetic data generation method is then proposed to decrease data inhomogeneity and increase the accuracy of the predictions. For this purpose, a chemical kinetic mechanism is chosen to generate physics-based synthetic data from 1D simulations. The final dataset is then prepared for the ML model training process. Finally, a hyperparameter optimisation study is carried out on the chosen ML model.

2.1. Training dataset

The experimental LBV measurements of NH_3/air, H_2/air, and NH_3/H_2/air mixtures from the literature are provided in Table 1. The spherical flame method with a constant volume combustion chamber (CVCC-SF) has been the primary choice of measuring equipment for LBV. It can be noticed that there is insufficient experimental data in the literature, especially for elevated temperature and pressure conditions relevant to engine-operating conditions. Fig. 2 shows the year of publication for each experimental dataset, which reveals the increased interest in the NH_3/H_2/air blends as they offer great potential as zero-carbon fuels. Table 2 shows the ranges of experimental measurements provided in Table 1 as well as the total number of experimental data points. For initial ML model training, engine-relevant operating conditions are chosen as the following: ϕ = 0.6–1.7, p =

Table 1
Experimental LBV data collected from the literature.

Author(s)	Year	Method	X_{H_2}	ϕ	T_i (K)	P_i (MPa)
Hayakawa et al. [28]	2015	CVCC-SF	–	0.70–1.30	298	0.1–0.5
Takizawa et al. [29]	2008	CVCC-SF	–	0.89–1.20	298	0.1
Jabbour & Clodic [30]	2004	BM	–	0.90–1.30	298	0.1
Pfahl et al. [31]	2000	CVCC-SF	–	0.49–1.19	295	0.1
Ronney [32]	1988	CVCC-SF	–	0.58–1.79	300	0.1–0.2
Zakaznov et al. [33]	1979	BM	–	0.74–1.35	293	0.1
Mei et al. [34]	2019	CVCC-SF	–	0.70–1.30	298	0.1
Han et al. [35]	2020	HFB	–	0.85–1.25	298–448	0.1
Chen et al. [36]	2021	CVCC-SF	–	0.80–1.20	298	0.033–0.1
Lesmana et al. [37]	2022	BM	–	0.90–1.20	298	0.1
Ji et al. [38]	2021	CPCC-SF	–	0.60–2.00	303	0.1
Kanoshima et al. [39]	2022	CVCC-SF	–	0.80–1.20	400–500	0.1–0.5
Lee [40]	2010	CVCC-SF	0-0.5	0.60–1.67	298	0.1
Kumar [41]	2013	BM-CF	0.2–1.0	0.50–1.10	298	0.1
Li, J. et al. [42]	2014	BM-CF	0.33–0.6	0.60–1.40	298	0.1
Ichikawa et al. [43]	2015	CVCC-SF	0–1.0	1.00	298	0.1–0.5
Han et al. [44]	2019	HFB	0–0.4	0.70–1.60	298	0.1
Wang et al. [45]	2020	HFB	0.4–0.6	0.60–1.60	298	0.1–0.5
Lhuillier et al. [11]	2020	CVCC-SF	0–0.6	0.80–1.40	298–473	0.1
Shrestsha et al. [12]	2021	CVCC-SF	0–0.3	0.80–1.40	298–473	0.1–1.0
Gotama et al. [13]	2022	CVCC-SF	0–0.4	0.80–1.80	298	0.1–0.5
Li, H. et al. [46]	2022	CVCC-SF	0.2–1.0	0.80–1.40	298	0.05–0.2
Jin et al. [47]	2022	CVCC-SF	0.1–0.5	0.90–1.30	298–493	0.1–0.7
Chen et al. [48]	2023	CVCC-SF	0.0–1.0	0.50–1.50	298	0.05–0.15
Zhou et al. [49]	2023	CVCC-SF	0.0–0.7	0.70–1.40	298–423	0.1
Tse et al. [50]	2000	CB	1.0	0.50–4.00	298–443	0.1–6.0
Qin et al. [51]	2000	PTV	1.0	0.60–3.00	298	0.1
Kwon and Faeth [52]	2001	CVCC-SF	1.0	0.60–4.50	298	0.03–0.3
Pareja et al. [53]	2010	PTV	1.0	0.80–3.00	298	0.1
Liu and MacFarlane [54]	1983	BM	1.0	0.80–3.20	298	0.1
Wu and Law [55]	1985	BM	1.0	1.00–3.20	298	0.1
Gunther and Janisch [56]	1972	BM	1.0	0.80–3.20	298	0.1
Aung et al. [57]	1998	CVCC-SF	1.0	0.45–4.00	298	0.035–0.4
Lamoureux et al. [58]	2003	CVCC-SF	1.0	0.28–3.75	298	0.1
Dahoe et al. [59]	2005	CVCC-SF	1.0	0.50–3.00	293	0.1
Huang et al. [60]	2006	CVCC-SF	1.0	0.60–1.40	300	0.1
Hu et al. [61]	2009	CVCC-SF	1.0	0.40–4.50	303	0.1
Burke et al. [62]	2009	CB	1.0	1.50–4.50	298	0.1
Kuznetsov et al [63]	2012	CVCC-SF	1.0	0.28–4.50	285–295	0.025–0.1
Grossseuvre et al. [64]	2019	CVCC-SF	1.0	0.75–4.00	296–413	0.1
Dayma et al. [65]	2014	CVCC-SF	1.0	0.50–4.00	303	0.2–0.3
Krejci et al. [66]	2013	CVCC-SF	1.0	0.50-4.00‘	298–443	0.1–1.0
Sun and Li [67]	2016	CVCC-SF	1.0	0.50–4.00	300–450	0.1–0.5

Table 2
Experimental condition ranges for available literature data on LBV of NH_3/air, H_2/air, and NH_3/H_2/air mixtures.

Measurement	Range
Pressure (MPa)	0.025–10
Temperature (K)	295–500 K
Equivalence ratio (ϕ)	0.28–4.5
H_2 content (vol%)	0.0–100.0
LBV (cm/s)	2.1–443
No of experimental data	1178

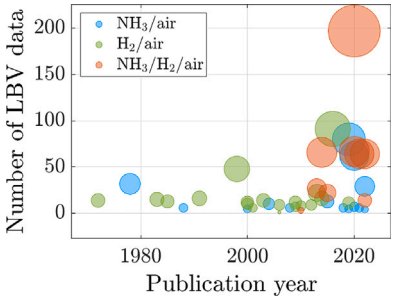

Fig. 2. Number of experimental data points with respect to the published year.

1–10 atm, T = 295–500 K and H_2 vol% contents of X_{H_2} = 0.0–1.0, and the rest of the data is discarded. Moreover, some experimental data points contain large uncertainty, especially near upper and lower flammability limits, and should be removed from the dataset. The process of removing outliers from a machine learning training dataset is essential in order to prevent the model from overfitting to extreme values, thereby improving its ability to generalise to new, unseen data. Therefore, experimental data points that contain an uncertainty more than 20% have been removed from the final experimental dataset to prevent outliers that may affect ML model training.

The final experimental dataset consisted of a 5 × 1178 matrix, in which the first four columns are the input parameters, namely, initial temperature (T_i), initial pressure (P_i), equivalence ratio (ϕ) and X_{H_2} and the fifth column is the output response, LBV. Experimental data distributions are shown in Fig. 3 with each point corresponding to an LBV measurement. Higher opacity indicates a higher number of data points at that experimental condition. It is prominent that certain conditions are not well-studied, and some conditions are not studied at all (e.g. $X_{H_2} > 0.6$ and $P_i > 5$ atm). This means that the ML algorithm must extrapolate for those unseen data points, introducing uncertainties. Furthermore, the data is highly skewed since the majority of the data comes from pure NH_3/air and H_2/air mixtures while NH_3/H_2/air mixtures, especially at high X_{H_2}, have not been well-studied. One solution is to generate synthetic data at these conditions to increase the homogeneity of the training dataset. This can be done using 1D

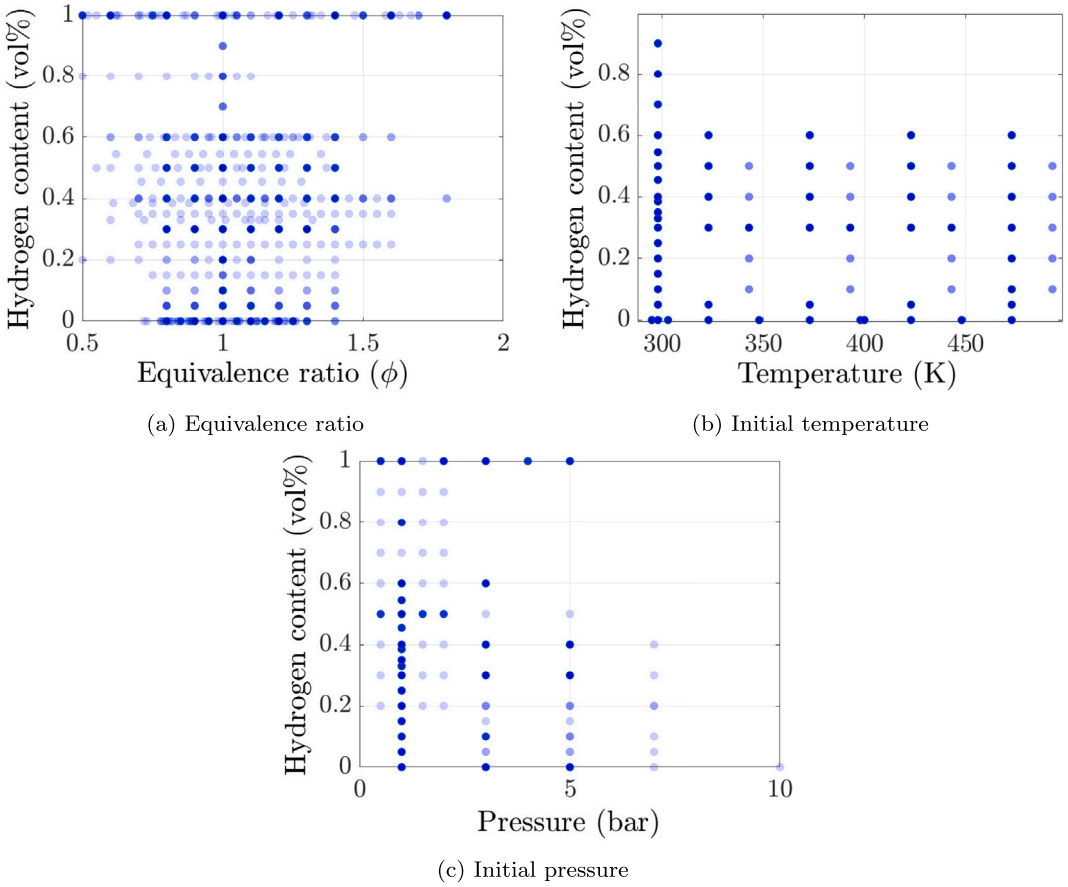

(a) Equivalence ratio

(b) Initial temperature

(c) Initial pressure

Fig. 3. Distribution of experimental LBV data for NH_3/air, H_2/air and NH_3/H_2/air mixtures based on temperature and pressure and equivalence ratio.

simulations that generate physics-based data points. Experimental and synthetic datasets can be merged to increase the predictive capability of the ML model.

2.2. Synthetic data generation

Mathematical i.e., glass-box models can be used to generate datasets for a specific machine learning application, this process is referred to as synthetic data generation. There are several reasons for applying this method, such as a limited number of data, time-intensive experiments and simulations, and experiment or simulation set-up costs. In this study, only a limited number of LBV experiments are available as shown in Fig. 3 and new experiments would require time, facility, and technical expertise. Therefore, an additional physics-based dataset is generated using 1D premixed flame simulations in Cantera [5] with a selected chemical kinetic mechanism as described in the following section.

2.2.1. Mechanism selection

Chemical kinetic mechanisms are usually tailored for certain combustion parameters such as ignition delay time (IDT), emissions and/or LBV for a range of conditions. A comparative study of mechanisms is required for this work since the target is to compute LBV for a wide range of P_i, T_i, ϕ and X_{H_2} conditions. Recently, Yin et al. [68] investigated several mechanisms for NH_3/H_2/air combustion and compared the error functions produced by each mechanism. It was seen that the Stagni [69], Zhang [70], Shrestha [12] and Han [71] produce almost the same amount of error function value. In our study, four recently developed mechanisms of similar sizes, namely Han [71], Gotama [13], Zhang [70] and Stagni [69] mechanisms, are chosen for a comparative assessment to find the best suited mechanism (See Table 3).

The focus is on NH_3/H_2/air blends since sufficient data is available for NH_3/air and H_2/air mixtures. Fig. 4 demonstrates the LBVs computed by selected mechanisms against the experimental data from different sources. Fig. 4(a) compares LBVs for NTP conditions with a $X_{H_2} = 0.6$ and there is a noticeable discrepancy between experiments, especially for near-stoichiometric conditions. When recent measurements by Wang et al. [45] and Lhuillier et al. [11] are taken into account, Gotama, Zhang and Han mechanisms perform well. Fig. 4(b) compares LBVs for 5 atm, 298 K and $X_{H_2} = 0.4$ conditions and large discrepancies ($\epsilon_{max} < 39\%$) are present for stoichiometric and rich conditions. It is seen that the Gotama mechanism outperforms other mechanisms. Finally, Fig. 4(c) shows the T_i dependencies of selected mechanisms. In this case, Han mechanism tends to underpredict LBVs by a margin ($\epsilon_{max} < 13\%$), especially for lean conditions. The Stagni mechanism tends to overpredict lean and near-stoichiometric conditions while performing well for rich conditions. On the other hand, lean and stoichiometric conditions are well predicted by the Gotama and Zhang mechanisms while rich conditions are slightly underpredicted. Overall, the Gotama mechanism performs reasonably well ($\epsilon_{max} < 10\%$) for the chosen conditions and is thus chosen for synthetic data generation.

2.2.2. 1D simulations

Laminar burning velocity (LBV) computations are carried by 1D freely propagating premixed flame i.e., "FreeFlame" simulations with Cantera [5]. For all simulations, multi-component formulation of the transport model, Soret diffusion effects, radiation effects, and tight convergence parameters (curve ≤ 0.05, slope ≤ 0.05, and ratio ≤ 3) are employed. For each simulation, up to 2000 grid points are used. The chemical kinetic mechanism by Gotama is used to carry out 1D simulations as it is comparatively assessed and validated for a wide

Table 3
Chemical kinetic mechanisms chosen for comparative study.

Mechanism	Year	Species	Reactions	Application targets
Stagni [69]	2020	31	210	Low-temperature (T < 1200 K) combustion of diluted NH_3/air
Han [71]	2021	36	298	LBV and self-ignition of NH_3/O_2 and H_2/H_2O mixtures
Zhang [70]	2021	39	264	NH_3 combustion and NO formation
Gotama [13]	2022	32	165	LBV of NH_3/H_2/air for fuel-rich and elevated pressure

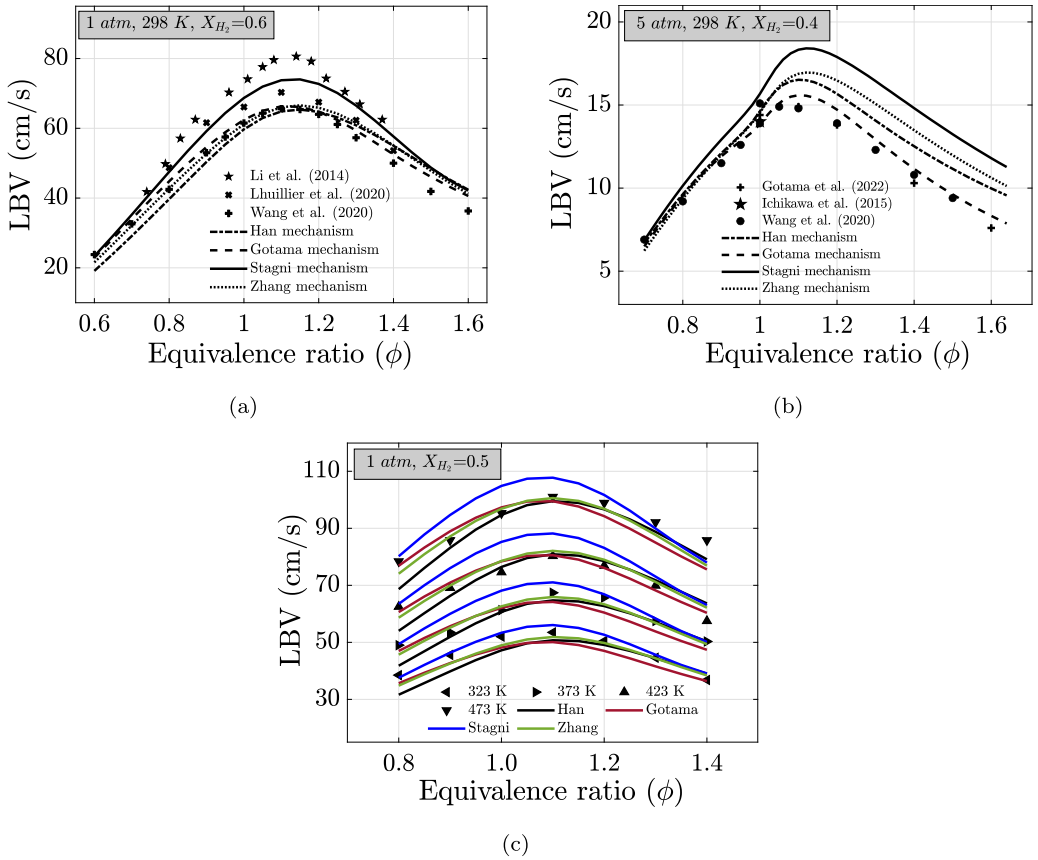

Fig. 4. Comparative mechanism validation study for (a) NTP and X_{H_2} = 0.6 (b) high P_i (5 atm) at 298 K and X_{H_2} = 0.4; (c) T_i dependency at P_i = 1 atm and X_{H_2} = 0.5.

range of conditions. Experimental conditions where no data is available are specifically targeted to increase the predictive capability of the ML model. These ranges are as follows: p = 3–10 atm, ϕ = 0.6–1.7, T = 295–500 K, X_{H_2} = 0.1 – 0.9 (especially focusing on 0.4–0.9 range). In total, additional 5890 LBV data points (five times the original experimental dataset size) are generated in given ranges of conditions to assess the dataset size dependency of the ML models.

2.3. Model training methodology

The goal is to first train the ML model using the experimental dataset and then increase the accuracy with the synthetic data (hybrid approach). The datasets need to be prepared for ML model training. Machine learning algorithms benefit from normalisation when the input data has variable scales. Normalisation improves the adaptation ability of ML algorithms and speeds up convergence. In this study, the variables have a scale difference of two orders of magnitude, and normalisation is required. Thus, normalisation to a range between 0.0–1.0 is carried out with the following formula:

$$z_i = \frac{x_i - \min(x)}{\max(x) - \min(x)} \tag{1}$$

where, x is the feature vector, x_i is the i_{th} element of feature vector and z_i is the normalised value of i_{th} element in the x vector. On the other hand, model response i.e., LBV distribution, is highly skewed (Fisher–Pearson coefficient of skewness = 2.02). Skewness can be addressed by applying a logarithmic transformation to the response variable, LBV, which then can be retransformed to evaluate the model with new data. The dependency of LBV on each independent input feature can be investigated with Pearson correlation matrix as shown in Fig. 5. When NH_3/air mixtures are investigated (Fig. 5(a)), T is strongly positively correlated with LBV. Whereas for H_2/air mixtures (Fig. 5(b)) ER (ϕ) has the highest correlation coefficient. Lastly, when NH_3/H_2/air mixtures are investigated (Fig. 5(c)), X_{H_2} has the highest correlation coefficient followed by initial temperature (T_i) while initial pressure (P_i) has a negative correlation.

Then, the dataset is randomly split into three sets: 70% for the training set (826 points), 15% for the validation set for cross-validation of models (176 points), 15% for the test set for testing of each model (176 points). A similar approach is also used for the hybrid case.

Since this is a multidimensional regression problem, appropriate regression algorithms, namely linear regression models (LR), regression trees (RT), support vector machines (SVM), gaussian process regression (GPR), ensembles of trees (ET) as well as neural networks (NN), are investigated for model predictive capability comparison. In total, 24 ML algorithms are evaluated which are the variations of the mentioned regression algorithms.

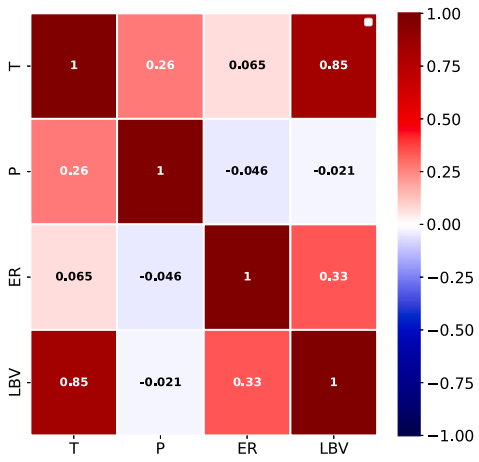

(a) NH_3/air

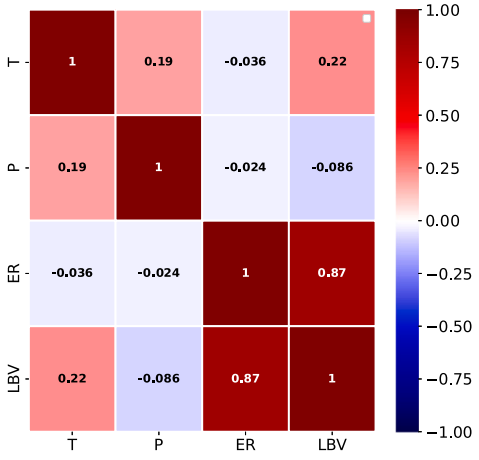

(b) H_2/air

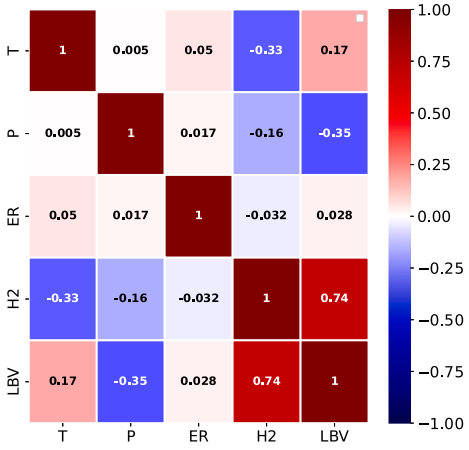

(c) NH_3/H_2/air

Fig. 5. Pearson correlation matrix based on the experimental dataset.

2.4. Model performance evaluation

The performance of each model is systematically assessed based on statistical metrics such as coefficient of determination (R^2), mean absolute error (MAE), and root mean square error (RMSE). These metrics are mathematically described in Eqs. (2)–(4);

$$RMSE = \sqrt{\frac{1}{m}\sum_{i=1}^{m}(LBV - \widehat{LBV})^2} \tag{2}$$

$$MAE = \frac{1}{m}\sum_{i=1}^{m}|(LBV - \widehat{LBV})| \tag{3}$$

$$R^2 = \frac{\left(\sum_{i=1}^{m}(LBV - \overline{LBV})(LBV - \overline{LBV})\right)^2}{\left(\sum_{i=1}^{m}(LBV - \overline{LBV})\sum_{i=1}^{m}(LBV - \overline{LBV})\right)^2} \tag{4}$$

2.5. Model validation and testing

Model validation is of paramount importance in any ML study, as it ensures that the model generalises well. Cross-validation approach prevents the model to be dependent on the specific set of training and validation data and ensures a global predictive performance evaluation. In this study, k-fold cross-validation approach [72] is applied to validate the model. In k-fold cross-validation approach, dataset is split into k number of folds (in this case k = 10) for an iterative training process. Each fold consists of a training and a validation set which is varied for each iteration as shown in Fig. 6. Therefore, in each iteration, the prediction accuracy of the model is tested for corresponding validation set in for each individual fold. The overall error of the model is obtained by averaging the errors of all folds as given in Eq. (5).

$$\mathrm{Err}_{\mathrm{mean}} = \frac{1}{\mathrm{k}}\sum_{i=1}^{\mathrm{k}}\mathrm{Err}_i \tag{5}$$

2.6. Model hyperparameter optimisation

A regression machine learning algorithm, A, maps a set $d_1,d_2,\ldots,d_n$ of data points $D = (x_i,y_i)$ to a function that is written as a vector of model parameters. In this problem, x_i are the input features and y_i is the output response of the model while θ is the parameter set. Machine learning algorithms use hyperparameters, $\theta \epsilon \Lambda$, which affect the functioning of learning algorithm A_θ. These hyperparameters can be optimised in a loop that evaluates the effect of each hyperparameter

Table 4
ML model evaluation results.

ML algorithms		R^2		MAE (cm/s)		RMSE (cm/s)		Speed-up (t_{1D}/t_{ML})
		Exp	Hybrid	Exp	Hybrid	Exp	Hybrid	
LR	Simple	0.838	0.941	22.32	14.00	24.81	15.68	26 000–27 000
	Stepwise	0.873	0.962	19.34	12.94	21.02	14.67	
	Robust	0.838	0.942	22.11	13.93	24.54	15.68	
	Interactions	0.873	0.962	19.60	12.92	21.20	14.67	
RT	Coarse	0.889	0.959	18.99	13.07	20.82	14.84	24 000–26 000
	Medium	0.925	0.972	16.88	11.11	19.74	12.76	
	Fine	0.953	0.982	13.34	9.95	15.54	11.50	
SVM	Linear	0.829	0.942	23.10	13.91	24.95	15.71	22 000–24 000
	Quadratic	0.940	0.942	13.71	13.98	15.67	10.15	
	Cubic	0.954	0.992	12.84	7.11	14.52	8.84	
	Coarse Gaussian	0.932	0.989	15.01	8.37	16.98	9.84	
	Medium Gaussian	0.957	0.992	13.29	7.52	16.05	8.66	
	Fine Gaussian	0.841	0.986	21.97	9.45	23.88	10.75	
GPR	Rational quadratic	0.972	0.997	11.32	4.42	13.30	7.02	18 000–20 000
	Matern 5/2	**0.983**	**0.998**	**9.62**	**4.24**	**11.44**	**6.92**	
	Exponential	0.976	0.997	10.22	4.30	12.63	7.02	
	Squared exponential	0.981	0.996	10.01	4.59	12.05	7.02	
ET	Boosted	0.935	0.957	16.20	13.13	18.23	14.52	24 000–26 000
	Bagged	0.932	0.989	15.98	8.75	18.03	10.10	
NN	Bilayered	0.986	0.995	9.21	5.42	11.04	8.90	9500–11 000
	Trilayered	0.988	0.995	9.02	5.40	10.80	7.19	
	Narrow	0.976	0.990	10.11	8.15	11.98	7.59	
	Medium	0.984	0.995	9.46	5.18	11.92	7.10	
	Wide	0.986	0.997	9.17	4.40	10.87	7.01	

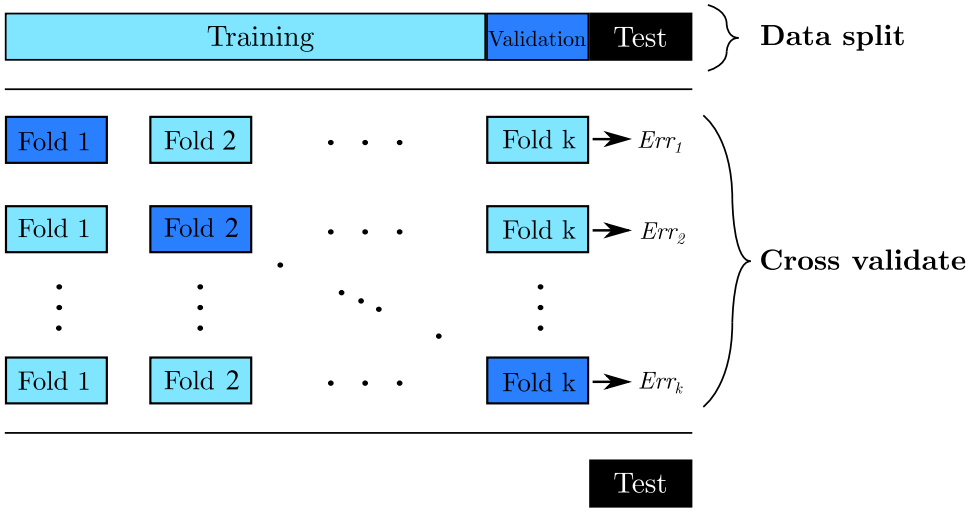

Fig. 6. Schematic overview of the k-fold cross-validation.

configuration using cross-validation [73]. The optimisation of hyperparameters of a ML algorithm, $\theta \in \mathbf{\Lambda}$, is somewhat a similar procedure to model selection. The goal here is to obtain the set of hyperparameters, $\theta^* \in \theta$, with the highest prediction accuracy. Considering n hyperparameters $\theta_1, \theta_2, \ldots, \theta_n \in \mathbf{\Lambda}$ with domains $\Lambda_1, \Lambda_2, \ldots, \Lambda_n$, a hyperparameter space, $\mathbf{\Lambda}$, can be obtained by taking cross-products of hyperparameters. Provided that there is a structured $\mathbf{\Lambda}$ space, the hyperparameter optimisation can be expressed as:

$$\theta^* \in \underset{\theta \in \mathbf{\Lambda}}{\operatorname{argmin}} \frac{1}{k} \sum_{i=1}^{k} \mathcal{L}\left(\mathrm{A}_k, \mathcal{D}_{\text{train}}, \mathcal{D}_{\text{validation}}\right) \tag{6}$$

where, $\mathcal{L}\left(\mathrm{A}_k, \mathcal{D}_{\text{train}}, \mathcal{D}_{\text{validation}}\right)$ is the loss attained by A whilst trained on $\mathcal{D}_{\text{train}}$ and assessed on $\mathcal{D}_{\text{validation}}$.

The details of the optimisation procedure for the chosen ML model is discussed in Section 3.2.

3. Results and discussion

3.1. ML algorithm selection

Table 4 lists the ML models together with their performance in predicting LBV values of the test datasets of both experimental and hybrid models. Generally, the model with the highest value of R^2 and the lowest MAE, and RMSE values is considered the best ML model. It was found that the GPR-Matern 5/2 model exhibits the smallest values of RMSE and MAE among all models, meanwhile, it also has the highest value of R^2, indicating this method can well capture the LBV of the test dataset. Overall, GPR and NN models performed well, achieving $R^2 > 99\%$ value, and could be further optimised (fine tuning) based on hyperparameters. Additionally, ML model is at least 9500 times faster (up to 27 000 times) in calculation time than the 1D simulations with the Gotama mechanism.

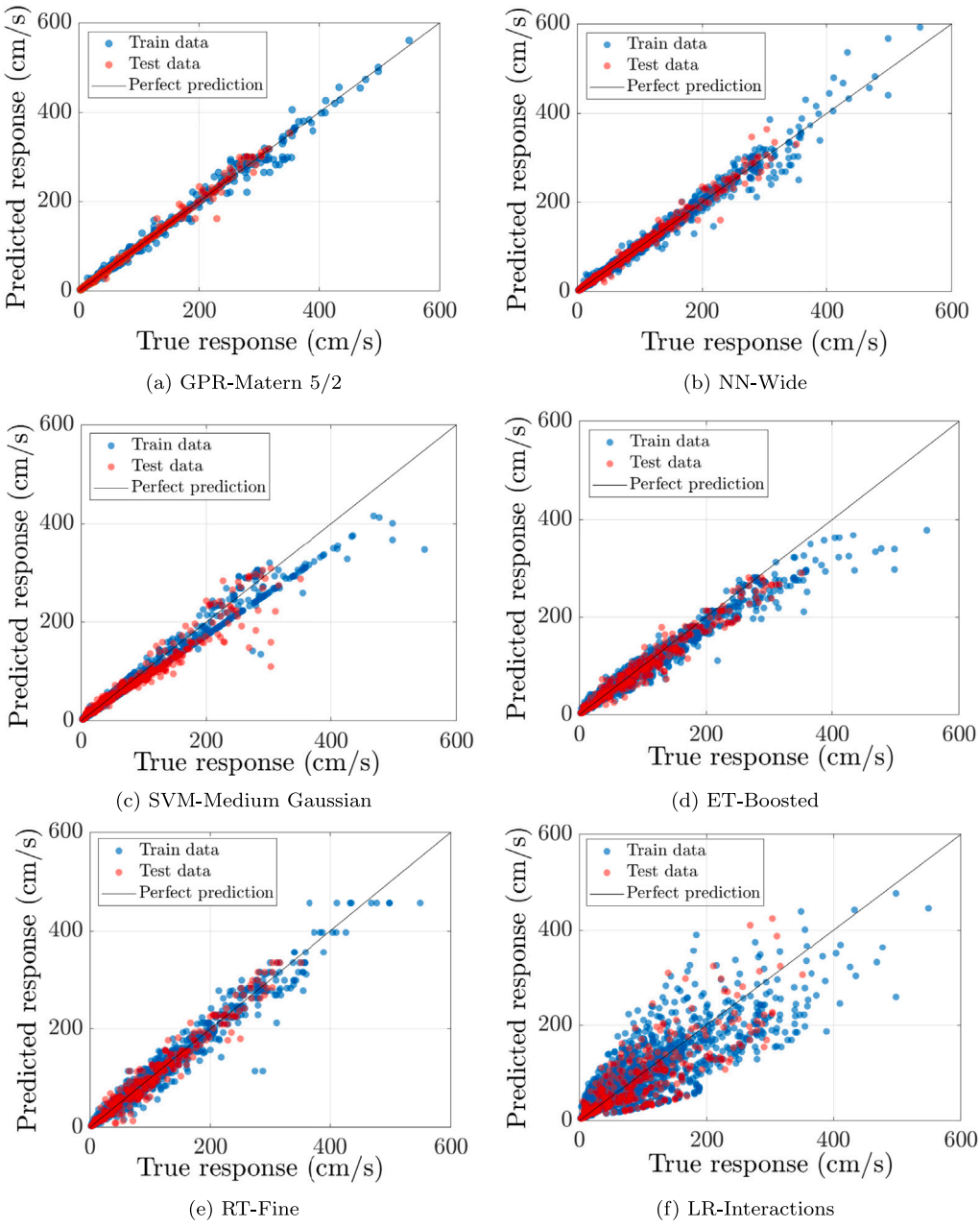

Fig. 7. Predicted LBV values versus true values from experiments and 1D simulations for training and test datasets.

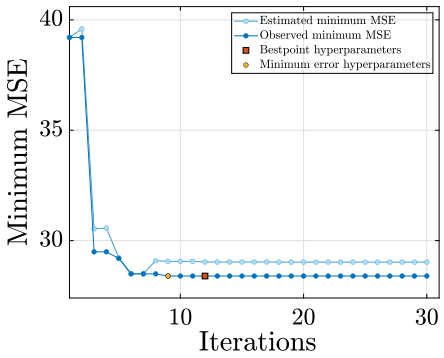

Fig. 8. Optimisation process of the chosen GPR-Matern 5/2 ML model.

Fig. 7 demonstrates a comparison of the model performances for both training and test datasets. It can be seen that the GPR-Matern 5/2 model (Fig. 7(a)) shows a good predictive capability as the predictions are concentrated along the perfect prediction line (y = x). It is also seen that the NN-Wide model (Fig. 7(b)) performs almost as good as the GPR-Matern 5/2 model. Finally, it is seen that even the best LR model (Fig. 7(f)) performs poorly and, therefore, should not be the primary choice of algorithm for complex, multi-variable problems such as LBV prediction.

Certain advantages of GPRs and NNs over other algorithms played an important role in the accuracy of the predictions. GPRs have the advantage of learning from small datasets and offer uncertainty estimation if required. NNs, as the second-best model, have the ability to learn complex relationships, handle large and noisy datasets, and generalise well to unseen data.

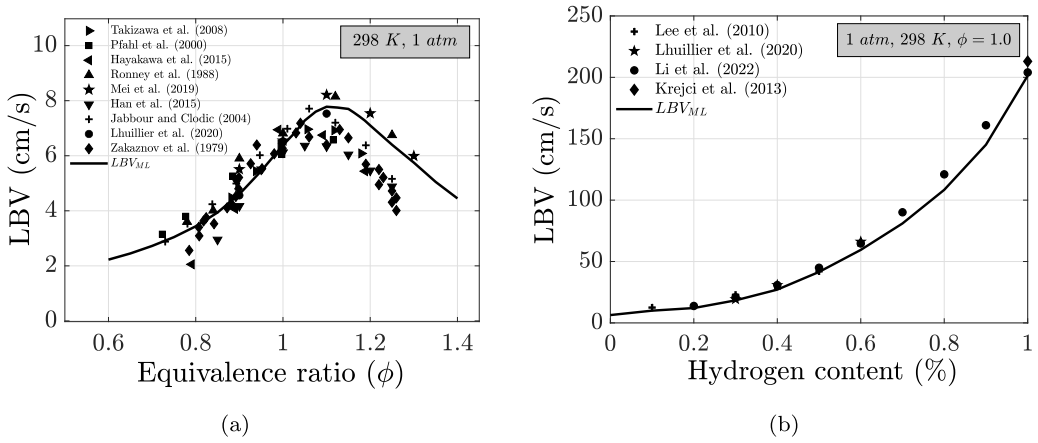

Fig. 9. Comparison of optimised ML model predictions with the experimental data (a) NH_3/air mixture at NTP. (b) Stoichiometric NH_3/H_2/air mixture at NTP.

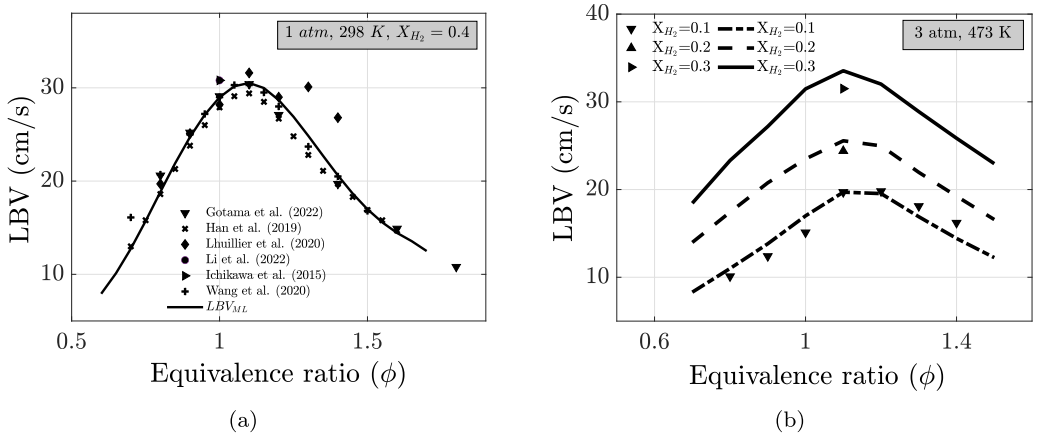

Fig. 10. Comparison of optimised ML model (GPR) predictions with the experimental data for NH_3/H_2/air mixtures (a) under NTP conditions and X_{H_2} = 0.4 [11,13,43–46] (b) P_i = 3 atm and T_i = 473 K [12].

3.2. Optimised ML model evaluation

The hyperparameters of GPR ML model that are chosen to be optimised are the basis function (Zero, Constant, and Linear), kernel function, and kernel scale. Bayesian optimisation is chosen as the optimiser. Fig. 8 shows the optimisation process of the GPR ML model based on the minimum mean-square error (MSE) of the model. The estimated minimum MSE is based on the upper confidence interval of the current MSE objective model whereas the observed minimum MSE is the computed value. The best point hyperparameters are the point that minimises an upper confidence interval of the MSE objective model. Minimum error hyperparameters correspond to the hyperparameters that result in the observed minimum MSE [74]. It can be seen that the model reaches the minimum MSE in 9 iterations and best point hyperparameters in 12 iterations and does not further improve. The optimisation process took 13.67 h on an 8-core 11th Gen Intel(R) Core(TM) i7-11800H 2.30 GHz and 16 GB RAM system. The final results showed that the optimised ML model achieves RMSE (cm/s) = 5.36, R^2 = 0.999, MAE (cm/s) = 1.80 and a prediction speed of approximately 12 000 observations per second.

The chosen model is further evaluated with new data to assess its prediction capabilities at various conditions. Fig. 9 shows the predictions of optimised ML model for pure NH_3/air mixtures and NH_3/H_2/air mixtures with increasing X_{H_2}. It is observed (Fig. 9(a)) that for pure NH_3/air mixture, optimised ML model predicts LBV well for lean and stoichiometric conditions while tends to overpredict for rich conditions (except Mei et al. [34]). It is seen in Fig. 9(b) that optimised ML model captures the X_{H_2} dependency profile of LBV very well with a slight underprediction ($\epsilon \approx 2.5\%$). It must be mentioned that the relative errors depend on the choice of the experimental dataset.

Fig. 10(a) shows the equivalence ratio dependency of optimised ML model at NTP and X_{H_2} = 0.4. This condition is intentionally chosen to compare the model to various experimental datasets. It is seen that the LBV profile is well captured for a wide range of equivalence ratios. Fig. 10(b) demonstrates LBV predictions for a relatively high temperature and moderate pressure condition (P_i = 3 atm and T_i = 473 K) where X_{H_2} is gradually increased. It is seen that the model performs well for these conditions and responds well to X_{H_2} changes.

3.3. Dataset size sensitivity analysis

The problem with ML is that the performance of trained models is highly dependent on the size of the dataset used. Fig. 11 shows the ensemble-averaged relative error ($\bar{\epsilon}(\%)$) profile with respect to training dataset size ($N_{training}$) to evaluate the sensitivity of current training architectures to the number of data points used in the training process. Here, x is the experimental dataset size (1178 points) and the first $\bar{\epsilon}$ shows the experimental data-based model error. It is seen that $\bar{\epsilon}$ follows almost an exponentially decreasing path. The threshold, $\bar{\epsilon} < 3\%$, is reached at a training dataset size of 5x and then $\bar{\epsilon}$ comes close to an asymptotic value of 2.5%.

4. Conclusion

In this work, an ML model was developed to predict LBV of NH_3/H_2/air mixtures for a wide range of conditions. Experimental LBV

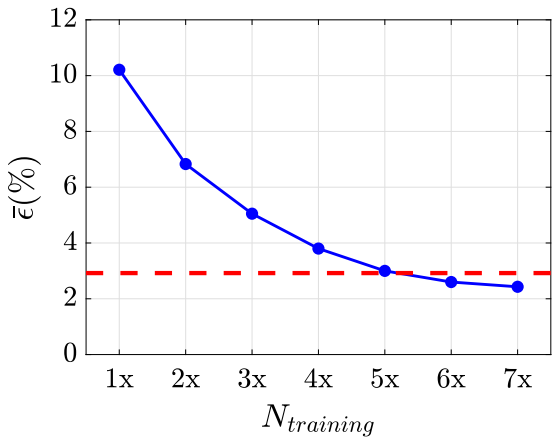

Fig. 11. Ensemble averaged relative error ($\bar{\epsilon}(\%)$) as a function of training dataset size ($N_{training}$) for GPR Matern 5/2 algorithm.

data were collected from the literature, processed, and normalised for ML training. Additionally, a synthetic data generation method using 1D premixed flame simulations was employed to generate additional LBV data points where there was a scarcity of experimental data. The new training dataset was integrated with the original experimental dataset using a hybrid approach, and the model was re-trained using 24 ML algorithms. From this study, the following conclusions can be drawn:

- Gotama mechanism outperforms Zhang, Han and Stagni mechanisms in prediction accuracy of LBVs for NH_3/H_2/air mixtures.
- The predictive capabilities of experimental data-based models can be increased via hybrid ML models using physics-based synthetic data.
- GPR and NN algorithms perform reasonably well (R^2 > 99%) in predicting LBV.
- The generalisation capability of the ML model can be improved by preventing overfitting using k-fold cross-validation and testing model accuracy with unseen data.
- Machine learning-based predictive models speed up the LBV calculation time by at least 9500 times and up to 27 000 times.

Given these conclusions, the ML models are seen as promising alternatives to time-consuming experimental measurements or numerical calculations of LBVs. For future work, the extrapolation ability of the model to higher pressures and temperatures is going to be studied. Additionally, the final optimised ML model is going to be integrated into an open-source CFD code to speed up the combustion modelling.

Declaration of competing interest

The authors declare that they have no known competing financial interests or personal relationships that could have appeared to influence the work reported in this paper.

Data availability

Data will be made available on request.

Acknowledgements

We gratefully acknowledge financial support by the Engineering and Physical Science Research Council (EPSRC) through the grant number EP/T033800/1.

References

[1] Kobayashi H, Hayakawa A, Somarathne KKA, Okafor EC. Science and technology of ammonia combustion. Proc Combust Inst 2019;37(1):109–33.
[2] Valera-Medina A, Xiao H, Owen-Jones M, David WI, Bowen P. Ammonia for power. Prog Energy Combust Sci 2018;69:63–102.
[3] Valera-Medina A, Pugh D, Marsh P, Bulat G, Bowen P. Preliminary study on lean premixed combustion of ammonia-hydrogen for swirling gas turbine combustors. Int J Hydrogen Energy 2017;42(38):24495–503.
[4] Konnov AA, Mohammad A, Kishore VR, Kim NI, Prathap C, Kumar S. A comprehensive review of measurements and data analysis of laminar burning velocities for various fuel+air mixtures. Prog Energy Combust Sci 2018;68:197–267.
[5] Goodwin DG, Moffat HK, Speth RL. Cantera: An object-oriented software toolkit for chemical kinetics, thermodynamics, and transport processes. 2018.
[6] Kee RJ, Rupley FM, Miller JA. Chemkin-II: A Fortran chemical kinetics package for the analysis of gas-phase chemical kinetics. Tech. rep., Livermore, CA (United States): Sandia National Lab.(SNL-CA); 1989.
[7] Cuoci A, Frassoldati A, Faravelli T, Ranzi E. OpenSMOKE++: An object-oriented framework for the numerical modeling of reactive systems with detailed kinetic mechanisms. Comput Phys Comm 2015;192:237–64.
[8] Goldmann A, Dinkelacker F. Approximation of laminar flame characteristics on premixed ammonia/hydrogen/nitrogen/air mixtures at elevated temperatures and pressures. Fuel 2018;224:366–78.
[9] Pessina V, Berni F, Fontanesi S, Stagni A, Mehl M. Laminar flame speed correlations of ammonia/hydrogen mixtures at high pressure and temperature for combustion modeling applications. Int J Hydrogen Energy 2022;47(61):25780–94.
[10] Mathieu O, Petersen EL. Experimental and modeling study on the high-temperature oxidation of Ammonia and related NOx chemistry. Combust Flame 2015;162(3):554–70.
[11] Lhuillier C, Brequigny P, Lamoureux N, Contino F, Mounaïm-Rousselle C. Experimental investigation on laminar burning velocities of ammonia/hydrogen/air mixtures at elevated temperatures. Fuel 2020;263:116653.
[12] Shrestha KP, Lhuillier C, Barbosa AA, Brequigny P, Contino F, Mounaïm-Rousselle C, Seidel L, Mauss F. An experimental and modeling study of ammonia with enriched oxygen content and ammonia/hydrogen laminar flame speed at elevated pressure and temperature. Proc Combust Inst 2021;38(2):2163–74.
[13] Gotama GJ, Hayakawa A, Okafor EC, Kanoshima R, Hayashi M, Kudo T, Kobayashi H. Measurement of the laminar burning velocity and kinetics study of the importance of the hydrogen recovery mechanism of ammonia/hydrogen/air premixed flames. Combust Flame 2022;236:111753.
[14] Otomo J, Koshi M, Mitsumori T, Iwasaki H, Yamada K. Chemical kinetic modeling of ammonia oxidation with improved reaction mechanism for ammonia/air and ammonia/hydrogen/air combustion. Int J Hydrogen Energy 2018;43(5):3004–14.
[15] Zhou L, Song Y, Ji W, Wei H. Machine learning for combustion. Energy AI 2022;7:100128.
[16] Williams Z, Moiz A, Cung K, Smith M, Briggs T, Bitsis C, Miwa J. Generation of Rate-of-Injection (ROI) profile for Computational Fluid Dynamics (CFD) model of Internal Combustion Engine (ICE) using machine learning. Energy and AI 2022;8:100148.
[17] Ihme M, Chung WT, Mishra AA. Combustion machine learning: Principles, progress and prospects. Prog Energy Combust Sci 2022;91:101010.
[18] Nguyen H-T, Domingo P, Vervisch L, Nguyen P-D. Machine learning for integrating combustion chemistry in numerical simulations. Energy AI 2021;5:100082.
[19] Mehra RK, Duan H, Luo S, Ma F. Laminar burning velocity of hydrogen and carbon-monoxide enriched natural gas (HyCONG): An experimental and artificial neural network study. Fuel 2019;246:476–90.
[20] Malik K, Żbikowski M, Teodorczyk A. Laminar burning velocity model based on deep neural network for hydrogen and propane with air. Energies 2020;13(13):3381.
[21] Ambrutis A, Povilaitis M. Development of a CFD-suitable deep neural network model for laminar burning velocity. Appl Sci 2022;12(15):7460.
[22] Malet F. Numerical and experimental study of premixed turbulent hydrogen flame propagation in lean and wet atmosphere. Tech. rep., Orleans Univ.; 2005.
[23] vom Lehn F, Cai L, Cáceres BC, Pitsch H. Exploring the fuel structure dependence of laminar burning velocity: A machine learning based group contribution approach. Combust Flame 2021;232:111525.
[24] Eckart S, Prieler R, Hochenauer C, Krause H. Application and comparison of multiple machine learning techniques for the calculation of laminar burning velocity for hydrogen-methane mixtures. Therm Sci Eng Prog 2022;32:101306.
[25] Wan Z, Wang Q-D, Wang B-Y, Liang J. Development of machine learning models for the prediction of laminar flame speeds of hydrocarbon and oxygenated fuels. Fuel Commun 2022;12:100071.
[26] Varghese RJ, Kolekar H, Kumar S. Laminar burning velocities of H2/CO/CH4/CO2/N2-air mixtures at elevated temperatures. Int J Hydrogen Energy 2019;44(23):12188–99.

[27] Shahpouri S, Norouzi A, Hayduk C, Fandakov A, Rezaei R, Koch CR, Shahbakhti M. Laminar flame speed modeling for low carbon fuels using methods of machine learning. Fuel 2023;333:126187.
[28] Hayakawa A, Goto T, Mimoto R, Arakawa Y, Kudo T, Kobayashi H. Laminar burning velocity and Markstein length of ammonia/air premixed flames at various pressures. Fuel 2015;159:98–106.
[29] Takizawa K, Takahashi A, Tokuhashi K, Kondo S, Sekiya A. Burning velocity measurements of nitrogen-containing compounds. J Hard Mater 2008;155(1–2):144–52.
[30] Jabbour T, Clodic DF. Burning velocity and refrigerant flammability classification/discussion. ASHRAE Trans 2004;110:522.
[31] Pfahl U, Ross M, Shepherd J, Pasamehmetoglu K, Unal C. Flammability limits, ignition energy, and flame speeds in H2–CH4–NH3–N2O–O2–N2 mixtures. Combust Flame 2000;123(1–2):140–58.
[32] Ronney PD. Effect of chemistry and transport properties on near-limit flames at microgravity. Combust Sci Technol 1988;59(1–3):123–41.
[33] Zakaznov V, Kursheva L, Fedina Z. Determination of normal flame velocity and critical diameter of flame extinction in ammonia-air mixture. Combust Explos Shock Waves 1978;14(6):710–3.
[34] Mei B, Zhang X, Ma S, Cui M, Guo H, Cao Z, Li Y. Experimental and kinetic modeling investigation on the laminar flame propagation of ammonia under oxygen enrichment and elevated pressure conditions. Combust Flame 2019;210:236–46.
[35] Han X, Wang Z, He Y, Zhu Y, Cen K. Experimental and kinetic modeling study of laminar burning velocities of NH3/syngas/air premixed flames. Combust Flame 2020;213:1–13.
[36] Chen X, Liu Q, Jing Q, Mou Z, Shen Y, Huang J, Ma H. Flame front evolution and laminar flame parameter evaluation of buoyancy-affected ammonia/air flames. Int J Hydrogen Energy 2021;46(77):38504–18.
[37] Lesmana H, Zhu M, Zhang Z, Gao J, Wu J, Zhang D. Experimental and kinetic modelling studies of laminar flame speed in mixtures of partially dissociated NH3 in air. Fuel 2020;278:118428.
[38] Ji C, Wang Z, Wang D, Hou R, Zhang T, Wang S. Experimental and numerical study on premixed partially dissociated ammonia mixtures. Part I: Laminar burning velocity of NH3/H2/N2/air mixtures. Int J Hydrogen Energy 2022;47(6):4171–84.
[39] Kanoshima R, Hayakawa A, Kudo T, Okafor EC, Colson S, Ichikawa A, Kudo T, Kobayashi H. Effects of initial mixture temperature and pressure on laminar burning velocity and Markstein length of ammonia/air premixed laminar flames. Fuel 2022;310:122149.
[40] Lee J, Kim J, Park J, Kwon O. Studies on properties of laminar premixed hydrogen-added ammonia/air flames for hydrogen production. Int J Hydrogen Energy 2010;35(3):1054–64.
[41] Kumar P, Meyer TR. Experimental and modeling study of chemical-kinetics mechanisms for H2–NH3–air mixtures in laminar premixed jet flames. Fuel 2013;108:166–76.
[42] Li J, Huang H, Kobayashi N, He Z, Nagai Y. Study on using hydrogen and ammonia as fuels: Combustion characteristics and NOx formation. Int J Energy Res 2014;38(9):1214–23.
[43] Ichikawa A, Hayakawa A, Kitagawa Y, Somarathne KKA, Kudo T, Kobayashi H. Laminar burning velocity and Markstein length of ammonia/hydrogen/air premixed flames at elevated pressures. Int J Hydrogen Energy 2015;40(30):9570–8.
[44] Han X, Wang Z, Costa M, Sun Z, He Y, Cen K. Experimental and kinetic modeling study of laminar burning velocities of NH3/air, NH3/H2/air, NH3/CO/air and NH3/CH4/air premixed flames. Combust Flame 2019;206:214–26.
[45] Wang S, Wang Z, Elbaz AM, Han X, He Y, Costa M, Konnov AA, Roberts WL. Experimental study and kinetic analysis of the laminar burning velocity of NH3/syngas/air, NH3/CO/air and NH3/H2/air premixed flames at elevated pressures. Combust Flame 2020;221:270–87.
[46] Li H, Xiao H, Sun J. Laminar burning velocity, Markstein length, and cellular instability of spherically propagating NH3/H2/Air premixed flames at moderate pressures. Combust Flame 2022;241:112079.
[47] Jin B-z, Deng Y-F, Li G-x, Li H-m. Experimental and numerical study of the laminar burning velocity of NH3/H2/air premixed flames at elevated pressure and temperature. Int J Hydrogen Energy 2022;47(85):36046–57.
[48] Chen X, Liu Q, Zhao W, Li R, Zhang Q, Mou Z. Experimental and chemical kinetic study on the flame propagation characteristics of ammonia/hydrogen/air mixtures. Fuel 2023;334:126509.
[49] Zhou S, Cui B, Yang W, Tan H, Wang J, Dai H, Li L, ur Rahman Z, Wang X, Deng S, et al. An experimental and kinetic modeling study on NH3/air, NH3/H2/air, NH3/CO/air, and NH3/CH4/air premixed laminar flames at elevated temperature. Combust Flame 2023;248:112536.
[50] Tse SD, Zhu D, Law CK. Morphology and burning rates of expanding spherical flames in H2/O2/inert mixtures up to 60 atmospheres. Proc Combust Inst 2000;28(2):1793–800.
[51] Qin X, Kobayashi H, Niioka T. Laminar burning velocity of hydrogen–air premixed flames at elevated pressure. Exp Therm Fluid Sci 2000;21(1–3):58–63.
[52] Kwon O, Faeth G. Flame/stretch interactions of premixed hydrogen-fueled flames: measurements and predictions. Combust Flame 2001;124(4):590–610.
[53] Pareja J, Burbano HJ, Ogami Y. Measurements of the laminar burning velocity of hydrogen–air premixed flames. Int J Hydrogen Energy 2010;35(4):1812–8.
[54] Liu D, MacFarlane R. Laminar burning velocities of hydrogen-air and hydrogen-air steam flames. Combust Flame 1983;49(1–3):59–71.
[55] Wu CK, Law CK. On the determination of laminar flame speeds from stretched flames. In: Symposium (International) on combustion, Vol. 20. Elsevier; 1985, p. 1941–9.
[56] Günther R, Janisch G. Measurements of burning velocity in a flat flame front. Combust Flame 1972;19(1):49–53.
[57] Aung K, Hassan M, Faeth G. Effects of pressure and nitrogen dilution on flame/stretch interactions of laminar premixed H2/O2/N2 flames. Combust Flame 1998;112(1–2):1–15.
[58] Lamoureux N, Djebaıli-Chaumeix N, Paillard C-E. Laminar flame velocity determination for H2–air–He–CO2 mixtures using the spherical bomb method. Exp Therm Fluid Sci 2003;27(4):385–93.
[59] Dahoe A. Laminar burning velocities of hydrogen–air mixtures from closed vessel gas explosions. J Loss Prev Process Ind 2005;18(3):152–66.
[60] Huang Z, Zhang Y, Zeng K, Liu B, Wang Q, Jiang D. Measurements of laminar burning velocities for natural gas–hydrogen–air mixtures. Combust Flame 2006;146(1–2):302–11.
[61] Hu E, Huang Z, He J, Jin C, Zheng J. Experimental and numerical study on laminar burning characteristics of premixed methane–hydrogen–air flames. Int J Hydrogen Energy 2009;34(11):4876–88.
[62] Burke MP, Chen Z, Ju Y, Dryer FL. Effect of cylindrical confinement on the determination of laminar flame speeds using outwardly propagating flames. Combust Flame 2009;156(4):771–9.
[63] Kuznetsov M, Kobelt S, Grune J, Jordan T. Flammability limits and laminar flame speed of hydrogen–air mixtures at sub-atmospheric pressures. Int J Hydrogen Energy 2012;37(22):17580–8.
[64] Grosseuvres R, Comandini A, Bentaib A, Chaumeix N. Combustion properties of H2/N2/O2/steam mixtures. Proc Combust Inst 2019;37(2):1537–46.
[65] Dayma G, Halter F, Dagaut P. New insights into the peculiar behavior of laminar burning velocities of hydrogen–air flames according to pressure and equivalence ratio. Combust Flame 2014;161(9):2235–41.
[66] Krejci MC, Mathieu O, Vissotski AJ, Ravi S, Sikes TG, Petersen EL, Kérmonès A, Metcalfe W, Curran HJ. Laminar flame speed and ignition delay time data for the kinetic modeling of hydrogen and syngas fuel blends. J Eng Gas Turbines Power 2013;135(2).
[67] Sun Z-Y, Li G-X. Propagation characteristics of laminar spherical flames within homogeneous hydrogen-air mixtures. Energy 2016;116:116–27.
[68] Yin G, Xiao B, Zhao H, Zhan H, Hu E, Huang Z. Jet-stirred reactor measurements and chemical kinetic study of ammonia with dimethyl ether. Fuel 2023;341:127542.
[69] Stagni A, Cavallotti C, Arunthanayothin S, Song Y, Herbinet O, Battin-Leclerc F, Faravelli T. An experimental, theoretical and kinetic-modeling study of the gas-phase oxidation of ammonia. React Chem Eng 2020;5(4):696–711.
[70] Zhang X, Moosakutty SP, Rajan RP, Younes M, Sarathy SM. Combustion chemistry of ammonia/hydrogen mixtures: Jet-stirred reactor measurements and comprehensive kinetic modeling. Combust Flame 2021;234:111653.
[71] Han X, Lavadera ML, Konnov AA. An experimental and kinetic modeling study on the laminar burning velocity of NH3+N2O+air flames. Combust Flame 2021;228:13–28.
[72] Stone M. Cross-validatory choice and assessment of statistical predictions. J R Stat Soc Ser B Stat Methodol 1974;36(2):111–33.
[73] Hutter F, Kotthoff L, Vanschoren J. Automated machine learning: Methods, systems, challenges. Springer Nature; 2019.
[74] MathWorks I. MATLAB: the language of technical computing. Desktop tools and development environment, version 7, Vol. 9. MathWorks; 2005.